

MQP-BIO-DSA-5292  
MQP-BIO-DSA-5887  
MQP-BIO-DSA-8361

**MECHANISMS OF CELL DEATH CAUSED BY  
ENDOPLASMIC RETICULUM STRESS**

A Major Qualifying Project Report

Submitted to the Faculty of the

WORCESTER POLYTECHNIC INSTITUTE

in partial fulfillment of the requirements for the

Degree of Bachelor of Science

in

Biology and Biotechnology

By

---

Jared Broberg

---

Kyle Goodsell

---

Christopher Huston

April 26, 2012

APPROVED:

---

Fumihiko Urano, MD, PhD  
Program in Molecular Medicine  
UMASS Medical Center  
MAJOR ADVISOR

---

David Adams, PhD  
Biology and Biotechnology  
WPI Project Advisor

## ABSTRACT

Wolfram Syndrome is a rare genetic disorder, associated with optic nerve degeneration and diabetes mellitus. Most cases result from mutations in the WFS1 gene encoding *wolframin*, a negative regulator of ATF6 $\alpha$ . Our lab recently showed in pancreatic  $\beta$ -cells that mutated *wolframin* causes hyper activation of ATF6 $\alpha$  signaling which increases the protein unfolding response, leading to cell death. In this project, we tested various knockout and wild-type cell lines to distinguish which ER pathways are important to stress related apoptosis. The results showed that ATF6 $\alpha$ , which has previously been shown to increase ER stress in adult pancreatic cells, did not change cell death in embryonic mouse fibroblasts. However, the PERK and IRE1 $\alpha$  pathways are important in the cell death of embryonic mouse fibroblasts.

# TABLE OF CONTENTS

Signature Page .....	1
Abstract .....	2
Table of Contents .....	3
Acknowledgements .....	4
Background .....	5
Project Purpose .....	13
Methods .....	14
Results .....	21
Discussion .....	25
Bibliography .....	29

## **ACKNOWLEDGEMENTS**

We would like to thank our project sponsor and advisor Dr. Fumihiko Urano (UMMS) for allowing us to work in your laboratories and for all of your help throughout the project. Your knowledge and professional advice were paramount in helping us achieve our goal in being able to identify the mechanisms of cell death caused by endoplasmic reticulum stress. We would also like to thank all those who were able to assist us in the lab, including Kohsuke, Takashi, Marika Brian, Karen, and Victor, by giving us their insight, valuable perspective, and educational standpoint. We would like to thank our advisor Professor David Adams for providing us with comments, recommendations, and comprehensive feedback.

# BACKGROUND

## Wolfram Syndrome

Wolfram Syndrome is a rare genetic disorder that can crudely be defined as a neurodegenerative form of diabetes mellitus. It is first diagnosable by the development of diabetes mellitus at a young age. Its prevalence is low with around 1 in 500,000 children developing the disease (Barrett and Bundley, 1997). There is currently no cure.

### *Original Description*

The disease was first described in four siblings in 1938 by Drs. Don J. Wolfram and HP Wagener (Wolfram and Wagener, 1938). Wolfram and Wagner were studying eight siblings between the ages of 3 and 18 years, four of whom had developed diabetes mellitus and optic atrophy (Minton et al., 2003). These two symptoms are the most prevalent in Wolfram's patients and are the first to develop. The eldest of the four siblings developed diabetes mellitus at age 8 and optic atrophy at age 11; her brother had symptoms of vision loss at age 6 and developed diabetes mellitus at age 10. The two other siblings developed the same symptoms at similar ages, with diabetes mellitus developing at ages 7 and 5, and optic atrophy following a few years later (Barrett and Bundley, 1997). As the children aged the symptoms progressed with two of the siblings becoming almost completely blind and developing neurogenic bladders. Three of the four siblings had also lost some sense of hearing (Minton et al., 2003).

### ***Additional Cases***

Since the first description of this disease, there have only been around 200 additional recorded cases, so the disease is rare. The additional cases have provided additional symptoms including: diabetes insipidus (in which the kidneys cannot conserve water), renal out-flow tract abnormalities, and neurological and other endocrine abnormalities. The disease is also referred to as DIDMOAD (**D**iabetes **I**nsipidus, **D**iabetes **M**ellitus, **O**ptic **A**trophy, and **D**eafness). The average onset begins at age 6 with the development of diabetes mellitus. Next, optic atrophy begins at around 11 years old, and vision deteriorates culminating with blindness in most patients. At an average of 14 years, the majority of patients develop diabetes insipidus. Deafness begins to present around age 16. Other neurological and endocrine abnormalities also known to develop in patients are cerebral ataxia, peripheral neuropathy, psychiatric illness, hypogonadism, and renal tract irregularities. Ultimately, the disease leads to death around the age of 30. The most common reason for death is from respiratory failure resulting from degeneration of the brainstem (Rigoli et al., 2011).

### ***Wolfram Syndrome Genetics***

Wolfram's has been shown to be passed on through autosomal recessive inheritance (Barrett and Bundley, 1997). It often appears in siblings of the same family, but with no sign of the disease in the parents. The Wolfram's gene was first discovered in 1998 in a collaboration between an American/Japanese group (Inoue et al., 1998) and a group led by Dr. Tim Strom (Strom et al., 1998). The first group used positional cloning, and the latter group used a candidate gene approach, to identify a gene spanning 33.4 kb on the short arm of chromosome-4 (Rigoli et al., 2011). The gene was referred to as WFS1 by the Japanese group, and as *wolframin*

by Tim Strom's group. However, to prevent confusion with its protein, in this MQP report we will use WFS1 to refer to the gene, and *wolframin* to refer to the protein.

A second Wolfram's gene was identified in patients showing additional symptoms such as gastrointestinal bleeding, not seen in the earlier Wolfram's patients. After a study of sixteen blood related patients from Jordan who had these additional symptoms, scientists determined the cases were not linked to the WFS1 gene, but to a different locus on chromosome-4, known as WFS2 (Minton et al., 2003).

Mutations in WFS1 appear to cause the majority of Wolfram's cases (Rigoli et al., 2011), and WFS1 is the better characterized of the two Wolfram's genes. Patient screening has revealed several types of mutations in WFS1, including nonsense, missense, deletion, insertion, and frame shift mutations. The gene itself consists of 8 exons, with most cases showing a mutation in exon 8, which is significant for disease development. Translation of WFS1 produces a protein 890 amino acids long, known as *wolframin*. The protein is an endoglycosidase H-sensitive membrane glycoprotein with 9 transmembrane domains (Takeda et al., 2001). The protein has been found to be mainly localized in the endoplasmic reticulum (ER), especially of heart cells, brain, lungs, inner ear, and pancreas. Among its many functions, the ER is responsible for the folding and assembling of newly synthesized proteins. The role of *wolframin* in the ER is not yet fully understood, but current studies show that *wolframin* may play a role in the regulation of ER stress, and in turn cell survival. ER stress occurs when the function of the ER is disturbed, leading to a buildup of unfolded or misfolded proteins. *Wolframin* is believed to negatively regulate the protein "activating transcription factor 6 $\alpha$ " (ATF6 $\alpha$ ) which plays a crucial role in the unfolded protein response (Rigoli et al., 2011).

## The Unfolded Protein Response

Pancreatic  $\beta$ -cell death or dysfunction is one of the biggest contributors to hyperglycemia in individuals. In Wolfram patients, it is believed that ER stress plays a key role in the dysfunction and death of  $\beta$ -cells which leads to the hyperglycemia observed in diabetes mellitus (Osowski and Urano, 2010). When proteins begin to accumulate in the ER, or become misfolded, the ER becomes stressed. ER stress can be caused by hypoxia, oxidative injury, high fat diets, protein inclusion bodies, viral infection, or hypoglycemia among others. As a result of ER stress, the cell reacts by undergoing the unfolded protein response (UPR) which is a network of signaling pathways (**Figure 1**).

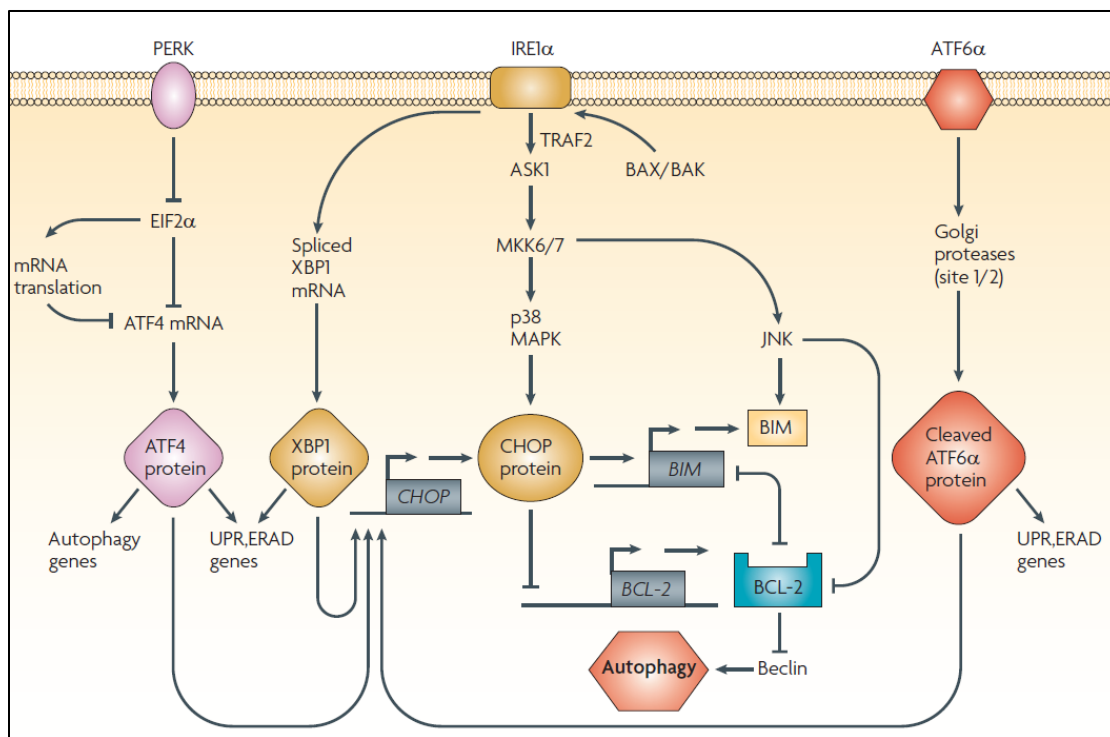


**Figure 1: Diagram of the Unfolded Protein Response (UPR) Pathway.** The figure depicts the network of signaling pathways involved in the UPR. The three pathways originate with the activation of transmembrane proteins IRE1 $\alpha$ , PERK, and ATF6 $\alpha$  (shown in the upper part of the figure) (Kim et al., 2008).

The excess proteins present during stress bind to chaperone proteins present in the ER which begin folding the proteins. This results in the release of specific transmembrane proteins into the ER lumen, which starts the UPR. The transmembrane proteins crucial for the initiation of the UPR are PRKR-like ER kinase (PERK), inositol-requiring kinase 1 (IRE1), and activating transcription factor 6 (ATF6 $\alpha$ ) (shown top left to right in the figure). Together these three transmembrane proteins increase the expression of ER chaperones, which can then try to ameliorate the accumulation of the misfolded proteins (Kim et al., 2008). Once the UPR is triggered, the pathway begins to undergo three effector functions: adaptation, alarm, and apoptosis. The initial response is to upregulate the expression of chaperones to aid in folding the accumulated proteins. If the cell has reached homeostasis after the upregulation of the chaperones, the UPR has a built in feedback response that will shut off the pathway (diagram center). If the accumulation continues and the stress is deemed unsolvable by the cell, it will enter apoptosis (Kim et al., 2008).

## IRE1

IRE1 is a type I transmembrane protein receptor that consists of an ER lumen domain, a transmembrane region, and a cytoplasmic domain, and is one of the key proteins in the activation of the unfolded protein response (UPR) (Lee et al., 2008). The different signal pathways that IRE1 activates are shown in Figure 1. IRE1 is required for the cleavage and post-transcriptional degradation of several different mRNAs that encode secreted proteins, for example insulin in  $\beta$ -cells. This mRNA cleavage and degradation reduces the load on the ER and thereby reduces some of the stress.

Another pathway that IRE1 is responsible for, which aids in the adaptation reaction of the UPR, involves its endoribonuclease domain. This domain processes an intron from the x-

box-binding protein 1 (XBP1) mRNA, allowing it to be translated to protein XBP1 (yellow in the figure), which forms a heterodimer with another protein called NF-Y. Together this new heterodimer complex is capable of promoting several different genes involved in the UPR (Kim et al., 2008).

If the ER stress conditions are unsolvable by other means, IRE1 is also able to activate apoptotic pathways. Under these conditions, IRE1 is able to work together with TNF receptor-associated-factor 2 (TRAF2) (diagram upper center) to activate protein kinases thought to aid in immunity, inflammation, and apoptosis (Kim et al., 2008). The most notable of these protein kinases is MAP3K5 (shown as MKK6/7 in the figure) which causes the activation of JNK (diagram center right). JNK (Jun N-terminal kinase) is an enzyme that when activated is able to aid in transcription, cell growth, oncogenic transformation, cell differentiation, and cell death (Weitzman, 2000).

## **PERK**

PERK is another one of the transmembrane proteins responsible for initiating the UPR pathways. Typically IRE1 is seen as the primary regulator of the pathway, and PERK is seen as the second in command. PERK is found abundantly in pancreatic  $\beta$ -cells and has been shown to have an effect on  $\beta$ -cell growth and proliferation (Oslowski and Urano, 2010). During the adaptation (effector) pathway of the UPR, PERK phosphorylates and inactivates eukaryotic translation initiation factor 2 $\alpha$  (EIF2 $\alpha$ ) (diagram upper left). The phosphorylation of EIF2 $\alpha$  results in the repression of protein translation. By limiting the translation of protein, PERK is able to slow the influx of new protein into the ER, which eases the burden (Hamanaka et al., 2005).

The phosphorylation of EIF2 $\alpha$  also stimulates the translation of several mRNAs that encode for short upstream open reading frames. Of these mRNAs is one encoding ATF4, a bZIP transcription factor (purple, diagram lower left). ATF4 is then either able to bind as a heterodimer with NRF2 to produce an antioxidant response, or to form a heterodimer with C/EBP to induce the transcription factor CHOP (yellow, diagram center). CHOP is then able to promote apoptosis of the cell by inhibiting a gene that encodes for an anti-apoptotic protein known as Bcl-2 (Schroder, 2006).

## ATF6 $\alpha$

ATF6 $\alpha$  is the third transmembrane protein responsible for initiating UPR pathway. Of the three transmembrane proteins, ATF6 $\alpha$  has been found to be the most associated with Wolfram Syndrome. ATF6 $\alpha$  protein is activated in a different way than either of the other two pathways. During ER stress, instead of activating other proteins through phosphorylation, the cytosol domain of ATF6 $\alpha$ , comprised of around 400 amino acids, is released and travels to the Golgi (Thuerlauf et al., 2004). Once in the Golgi, ATF6 $\alpha$  is cleaved, forming active transcription factor proteins that are transported to the nucleus where they upregulate the expression of genes responsible for protein folding, processing, and degradation. If ATF6 $\alpha$  becomes hyperactive due to an unsolvable accumulation of protein, it results in dysfunction and cell death. The specific effectors for this cell death pathway are currently not fully understood (Osowski and Urano, 2010).

Recently, scientists at the University of Massachusetts Medical School have discovered that the WFS1 gene is a key negative regulator of the UPR (Osowski and Urano, 2010). The group found that the *wolframin* protein encoded by WFS1 is integral in the regulation of ATF6 $\alpha$ .

*Wolframin* functions as a negative inhibitor in healthy cells by preventing the activation of ATF6 $\alpha$  signaling. During ER stress conditions, normal wild-type *wolframin* releases ATF6 $\alpha$  which allows it to go free and act as a transcription factor, as it normally would during ER stress. After the ER stress is mediated *wolframin* degrades the active ATF6 $\alpha$ . However, if the conformation of *wolframin* is changed due to a mutation, such as with Wolfram Syndrome patients, then ATF6 $\alpha$  escapes from *wolframin* degradation, and ATF6 $\alpha$  is always in a state of hyperactivation, which leads to death of the pancreatic  $\beta$ -cell (Osowski and Urano, 2010).

## **PROJECT PURPOSE**

The purpose of this project is to help identify which ER pathways are important in stress-related apoptosis. ER stress will be induced in embryonic mouse fibroblast cell lines using various toxins such as Tg and Tm, and the responses to the toxins will be measured by immunoblots for proteins related to apoptosis (such as caspase-2, caspase-3, caspase-9, and housekeeper GAPDH). The responses will be measured in knockout and WT cell lines for PERK, IRE1 $\alpha$ , ATF6 $\alpha$  transcription factor markers for key stress pathways.

# MATERIALS & METHODS

## Embryonic Mouse Fibroblast Cell Lines

Four different mouse embryonic fibroblast cell lines were used in this project: WT, ATF6 $\alpha$  KO, IRE1 $\alpha$  KO, and PERK KO. These cell lines were obtained from two different sources. The IRE1 $\alpha$  KO and PERK KO cell lines were acquired from David Ron at the University of Cambridge, and the ATF6 $\alpha$  KO cell line was acquired from Randal J. Kaufman at the Sanford-Burnham Medical Research Institute.

## Embryonic Mouse Fibroblast Cell Line Growth

All embryonic mouse fibroblasts were grown in DMEM 1X EAGLE's medium (Mediatech Inc.) supplemented with 10% FBS and 1% Penn-Strep. Cells were grown at 37°C in 5% CO<sub>2</sub> to confluency, then split. Trypsin-EDTA was used to remove the attached cells from the plate. The spent medium was aspirated, and the cells were rinsed with 10 mL of 1X PBS. The wash was aspirated, then 1.0 mL of Trypsin-EDTA was added. The flask was incubated at room temperature until the cells loosened from the bottom of the plate. Then, 10 mL of pre-warmed medium was added, and the cell suspension was centrifuged for 5 minutes at 1000 rpm. The supernatant was aspirated, and the cell pellet was re-suspended in 3 mL of pre-warmed medium. 1.0 mL of cell suspension was added to each of the three cell culture plates containing 9 ml of medium.

## Cell Plating into 12-Well Plates

The medium was aspirated from a confluent flask, and the flask rinsed with 10 ml of 1X PBS. The wash was aspirated, then 1 mL of Trypsin-EDTA was added to the attached cells. The flasks were left at room temperature for 1-2 minutes until the cells unattached. 10 mL of pre-warmed medium was added to the cell suspension, and the suspension was transferred to a 15mL conical tube and centrifuged for 5 minutes at 1000 rpm. The medium was aspirated, then the cell pellet was re-suspended in 10 mL of pre-warmed medium. 100  $\mu$ L of the cell suspension was mixed with an equal volume (100  $\mu$ L) of Trypan Blue Dye to make a dilution factor of 2. The mixture was pipetted up-and-down to mix, then 1  $\mu$ L of the solution was added onto a cell counting slide. The number of cells was counted in one of the grids, and the following equations were used to calculate the number of cells per mL, and to determine the volume containing  $3 \times 10^5$  cells per well:

Eq. 1: (# of cells in one grid) \* ( $10^4$ ) \* (dilution factor) = cells per mL in sample.  
For example, (45) \* ( $10^4$ ) \* (2) =  **$9.0 \times 10^6$  cells/mL**

Eq. 2: (Target # of cells) / (cells per mL in sample) = mL of cell solution to add per well. For example, ( $3 \times 10^5$ ) / (9,000,000) = **0.333 mL of cell solution to add per well.**

The volume corresponding to  $3 \times 10^5$  cells was added to each well of a 12-well microtiter plate, then pre-warmed medium was added to make a total volume of 1 mL. The plate was incubated 2 nights at 37°C in 5% CO<sub>2</sub>.

## Induction of ER Stress and Cell Harvesting

Two days after plating, the medium was aspirated from each well of the 12-well plate, and the cells were rinsed with 1 mL of 1XPBS. The wash was aspirated, and 1 mL of pre-

warmed medium was added to each well. A 1 mM stock solution of Thapsigargin (Tg) was diluted 1:100 (to make 10  $\mu$ M) by adding 1  $\mu$ L to 100  $\mu$ L of medium, and the solution was vortexed to mix. 10  $\mu$ L of the 10  $\mu$ M dilution was added to an appropriate well to make a final concentration of 0.1  $\mu$ M. Next, the 5 mg/mL Tunicamycin (Tm) stock solution was diluted 1:5000 (to make a 1  $\mu$ M dilution) by adding 1  $\mu$ L of the 5 mg/mL main stock solution to 50  $\mu$ L of medium. The mixture was vortexed to mix, then 10  $\mu$ L of the dilution was added to an appropriate well (to make a final concentration of 0.01  $\mu$ M). The microtiter dishes were incubated at 37°C for another 24 hours.

Following the 24 hr incubation, the spent medium was collected in a conical tube and the wells were washed with 1 mL of 1X PBS. The wash was also collected in the conical tube, then 0.2 mL of Trypsin-EDTA was added to each well to loosen the cells from the bottom of the wells. Once the cells loosened, 1 mL of pre-warmed medium was added to each well, and the cell suspension was transferred to the same conical tube as the old medium and the PBS wash. The tubes were centrifuged at 1000 rpm for 5 minutes, and the supernatant was aspirated, making sure to not aspirate the cell pellet at the bottom of the tube. 1 mL of 1X PBS was added to the cell pellet, and the tube was centrifuged again for 5 minutes at 1000 rpm. The wash was aspirated, and the cell pellet was re-suspended in 50  $\mu$ L of M-PER solution. The samples were frozen at -20°C for later use, or the protein concentration was determined (below).

### **Protein Concentration of Lysate Samples**

A 50  $\mu$ L cell lysate samples was defrosted, and the sample was transferred to a 1.5mL Eppendorf tube. The tube was centrifuged for 5 minutes at 1000 rpm to remove cell debris, and the supernatant was transferred to a new 1.5mL Eppendorf tube, making sure to leave the solid in

the old tube. The protein concentration was determined by comparison of an aliquot of the sample's absorbance at 280 nm compared to a sample of distilled water, which acted as the baseline with no protein present. The dilution required to produce a final protein concentration of 20  $\mu\text{g}/\mu\text{L}$  was calculated by using the Equation below:

$$\text{Eq. 3: } 20 \mu\text{g} / (\text{protein concentration in } \mu\text{g}/\mu\text{L}) = \text{target amount of lysate in } \mu\text{L}$$

For example:  $(20 \mu\text{g}) / (6.18 \mu\text{g}/\mu\text{L}) = \mathbf{3.2 \mu\text{L of sample needed.}}$

Once the appropriate concentrations and volumes were calculated, the amount of 4X Sample Buffer and distilled water needed to bring the sample to a total volume up to 25  $\mu\text{L}$  were determined. Mixed samples were either frozen for later use, or were immediately used for a Western Blot.

### **Western Blots**

Samples prepared as described above containing 20  $\mu\text{g}$  of protein in 25  $\mu\text{L}$  were placed on a 95°C heating block for 5 minutes to denature the protein. Tubes were briefly centrifuged to remove the condensation from the lid. A 5%-15% polyacrylamide gel (Biorad) was retrieved from 4°C storage, and the strip was removed from the bottom of the gel. The gel was placed into the electrophoresis unit with the smaller side of the glass facing the inside of the unit so the well labels can be read from outside. The comb was gently removed, making sure not to disrupt the wells. 1X Running Buffer was poured into the middle of the gel unit and on both sides so that the level was above the wells, making sure not to get the electrodes on top wet. 10  $\mu\text{L}$  of the Biorad Precision Protein Dual Color Standard marker was loaded into Lane 1 using a gel loading tip, making sure to record which lane the marker was placed in. The other wells were loaded

with the 25  $\mu$ L of the samples, making sure to label which sample was placed in each lane. The electrodes were connected to the apparatus, making sure to match up the colors. The gel was run at 30 amps (for one gel) or 60 amps (for 2 gels) for 30-60 min, or until the bromphenol blue dye reached the bottom of the gel.

While the gel was running, an ice pack was filled ice and water, and stored at  $-80^{\circ}\text{C}$ . Two fiber pads, 2 pieces of pre-cut filter paper, and a single PVDF membrane were obtained. The former two were soaked in 1X Transfer Buffer, while the PVDF membrane was soaked in methanol. Once the gel was done running, the gel was removed from the plate by using a special tool that came with the gel package. The wells were removed using a spatula, taking care not to rip the gel. The gel was placed in 1X Transfer Buffer. The immunoblot transfer apparatus was obtained and the gel sandwich was assembled on the black side of the cassette in the following order: First was placed a fiber pad, then a piece of filter paper, then the gel was carefully placed on top of the sandwich, again taking care not to rip the gel. Next, the the membrane was carefully placed onto the gel, taking care to have all of the samples on the gel covered by the membrane. The bubbles were cleared from the membrane, using the spatula to smooth the membrane. Next, a piece of filter paper was added, then finally the last fiber pad was added. The sandwich was clamped together, and the cassette inserted into the electrode module, making sure the black side is next to the black side of the electrode module. The icepack was retrieved, and placed on the open side of the apparatus. The tank was filled with 1X Transfer Buffer, and the electrodes were attached to the appropriate leads. The electroblot was run at 100 V for 60 minutes.

While the transfer was in progress, the blocking buffer was prepared by mixing 5 g of BSA or non-fat milk with 100 mL of TBST to make a 5% solution. Once the transfer was

complete, the sandwich was disassembled, and the membrane was placed in an immunoblot box with 10-20 mL of blocking solution. The box was rocked for 1 hour at room temperature, making sure the membrane could move back and forth in the box.

Once the blocking hour was completed, the blocking solution was dumped, and the membrane was washed 3 times using TBST, rocking for 5 minutes each time at room temperature. Enough TBST was used to completely cover the membrane and allow it to move. Once the washes were finished, they were discarded, and 10 mL of fresh blocking solution was added into the container, along with 10  $\mu$ L of primary antibody. The primary antibodies used were: GAPDH (CellSignaling 14C10, rabbit), Cleaved Caspase-3 (CellSignaling D175, 5A1E, rabbit), Caspase-2 (Millipore, rat), or Caspase-9 (CellSignaling, C9, mouse). Incubations with the primary antibodies were for overnight in the cold room.

The next day, the primary antibody solution was discarded, and the membrane was washed 3X with TBST as described above for 5 minutes each, then the membrane was placed in 10 mL of fresh blocking solution and 3  $\mu$ L of the appropriate secondary antibody was added to the solution, depending on which primary antibody was used. Secondary antibodies used were: HRP-conjugated anti-mouse IgG (CellSignaling), HRP-conjugated anti-rat IgG (CellSignaling), or HRP-conjugated anti-rabbit IgG (EBioScience). Incubations with secondary antibodies were at room temperature for 30 minutes on the rocker.

After the secondary antibody incubation, the membrane was washed 3X with TBST as described before, for 5 minutes each. Then 1 mL of fresh ECL Western Blotting Substrate (Pierce) was prepared for each membrane being visualized. The membranes were placed on a piece of plastic, and 1 mL of the solution was added and spread over each membrane. The membranes were incubated for 1 minute, then the membrane was lifted using tweezers and

placed between two plastic layers inside an Immunoblot Cassette, making sure to wipe away any excess drops of liquid. In the darkroom, one piece of x-ray film was placed into the cassette, and the film was exposed for 5 minutes. Sometimes the film was exposed longer if needed. The exposed film was placed inside the automatic film developer, and the button was pushed to feed the film into the machine.

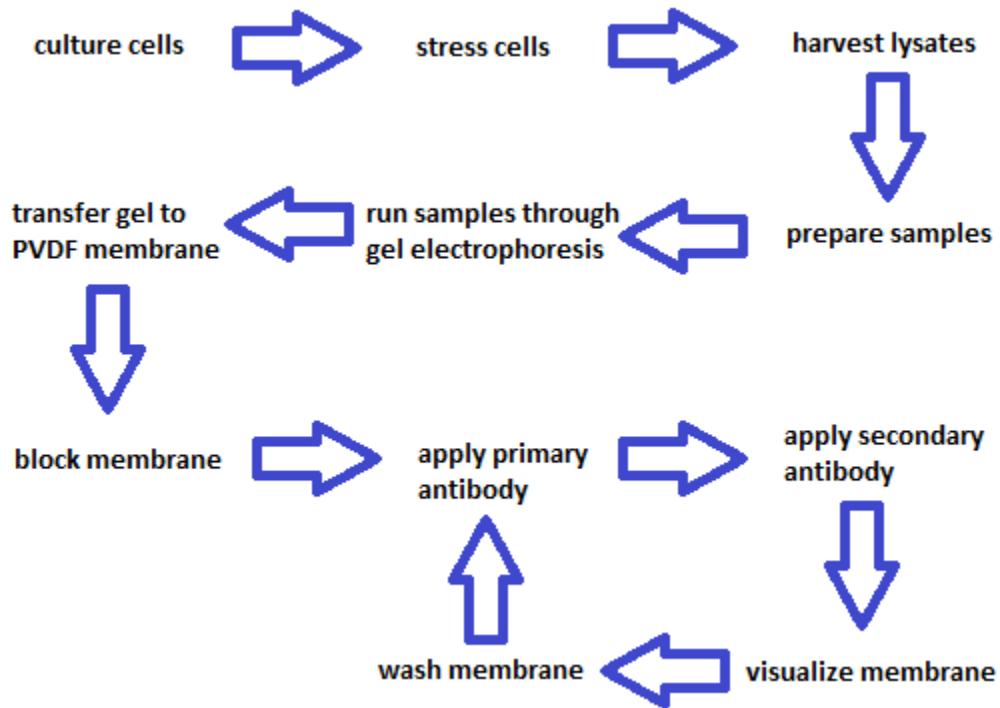


**Figure-2: Flow Chart of the Procedures Done for this Project.** This flow chart shows the general experimentation methods followed in this project. This approach was performed several times to attain multiple trials for each antibody. The antibodies used were for GAPDH (control), Caspase-3, Caspase-2 and Caspase-9.

## RESULTS

In this project, endoplasmic reticulum (ER) unfolded protein response (UPR) pathways resulting from ER stress were analyzed for their importance in embryonic fibroblast cells. Four different cell lines, three with different UPR pathways knocked out and a wild type control, were each treated with two different toxins (Tm or Tg) to induce ER stress. Once ER stress was induced, the cells were lysed and the levels of cleaved caspase-3 (a marker for apoptosis) were determined by immunoblots. GAPDH was used as a load marker. Caspase-3 was assayed because it is critical for apoptosis, and its cleavage is indicative of cell death. **Figures 3-7** below show the western blots for four separate trials. The four trials were performed to ensure the reproducibility of the results. In order to fit all of the samples into four gels an unusual ordering was used. The contents of each lane are explained in detail in each figure legend.

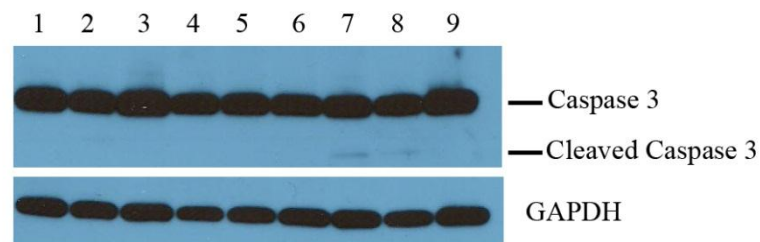


**Figure-3: First Half of Trial-1 for All Cell Lines.** Caspase-3 cleavage was observed in PERK-KO and IRE1 $\alpha$ -KO Tg treated cells. (1) Trial 1 WT untreated, (2) Trial 1 ATF6-KO untreated, (3) Trial 1 IRE1 $\alpha$ -KO untreated, (4) Trial 1 PERK-KO untreated, (5) Trial 1 WT Tg treated, (6) Trial 1 ATF6 $\alpha$ -KO Tg treated, (7) Trial 1 IRE1 $\alpha$ -KO Tg treated, (8) Trial 1 PERK-KO Tg treated, (9) Trial 3 WT untreated.

The first trial (**Figure-3**) showed capsase-3 cleavage in IRE1 $\alpha$ -KO (lane-7) and PERK-KO (lane-8) cell lines treated with Tg. The amount of capase-3 cleavage is small compared to the amounts of un-cleaved caspase-3. However, the presence of the cleaved caspase-3 shows

that cell death is occurring in these cells. **Figure-4** shows the second part of trial-1 (Tm samples only) and the first part of trial-2. Once again, the lanes loaded with trial-1 Tm-treated IRE1 $\alpha$ -KO (lane-3) and PERK-KO (lane-4) showed faint evidence of cleavage of caspase-3, however the equivalent samples for trial-2 (lanes-7 and 8) showed no cleaved caspase-3.

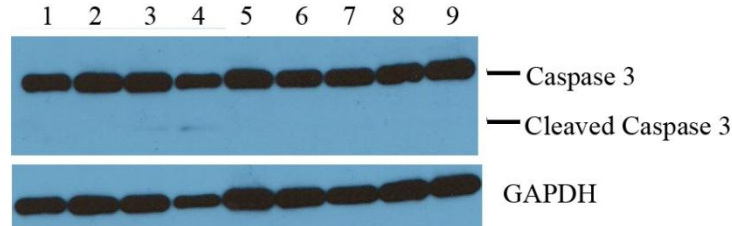


**Figure 4: Second Half of Trial-1 and First Half of Trial-2 for All Cell Lines.** Slight caspase-3 cleavage was observed in PERK-KO and IRE1 $\alpha$ -KO Tm treated cells. (1) Trial 1 WT Tm treated, (2) Trial 1 ATF6-KO Tm treated, (3) Trial 1 IRE1 $\alpha$ -KO Tm treated, (4) Trial 1 PERK-KO Tm treated, (5) Trial 2 WT untreated, (6) Trial 2 ATF6 $\alpha$ -KO untreated, (7) Trial 2 IRE1 $\alpha$ -KO untreated, (8) Trial 2 PERK-KO untreated, (9) Trial 3 ATF6 $\alpha$ -KO untreated.

The second half of trial-2 is shown in **Figure-5**. A slight caspase-3 cleavage was still observed in Tm-treated PERK-KO cells (lane-8) and Tg-treated IRE1 $\alpha$ -KO (lane-3), but no observable cleavage for Tm-IRE1 $\alpha$ -KO or Tg-PERK-KO as was seen in trial 1.

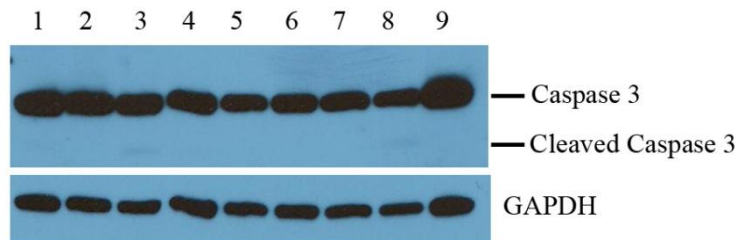


**Figure-5: Second Half of Trial-2 Results.** Very slight caspase-3 cleavage was observed in PERK-KO cells treated with Tm and IRE1 $\alpha$ -KO cells treated with Tg. (1) Trial 2 WT Tg treated, (2) Trial 2 ATF6-KO Tg treated, (3) Trial 2 IRE1 $\alpha$ -KO Tg treated, (4) Trial 2 PERK-KO Tg treated, (5) Trial 2 WT Tm treated, (6) Trial 2 ATF6 $\alpha$ -KO Tm treated, (7) Trial 2 IRE1 $\alpha$ -KO Tm treated, (8) Trial 2 PERK-KO Tm treated, (9) Trial 3 IRE1 $\alpha$ -KO untreated.

**Figure-6** shows the results for trial-3, which showed strong cleavage for Tm-IRE1 $\alpha$ -KO (lane-7) and Tm-PERK-KO (lane-8), but only slight or no cleavage for the equivalent Tg-treated samples.

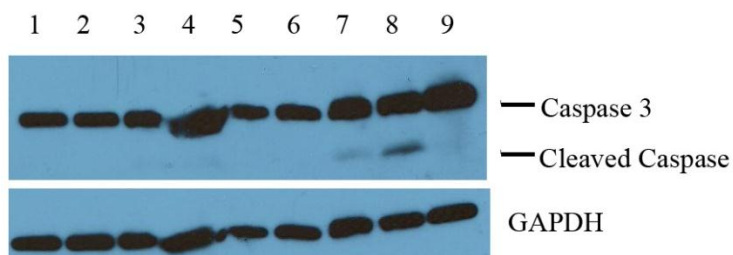


**Figure-6: Trial-3 Results.** Caspase-3 cleavage was observed in PERK-KO and IRE1 $\alpha$ -KO cells treated with Tm. (1) Trial 3 WT Tg treated, (2) Trial 3 ATF6-KO Tg treated, (3) Trial 3 IRE1 $\alpha$ -KO Tg treated, (4) Trial 3 PERK-KO Tg treated, (5) Trial 3 WT Tm treated, (6) Trial 3 ATF6 $\alpha$ -KO Tm treated, (7) Trial 3 IRE1 $\alpha$ -KO Tm treated, (8) Trial 3 PERK-KO Tm treated, (9) Trial 3 PERK-KO untreated.

After obtaining these results, a fourth trial was performed for just the PERK and IRE1 $\alpha$  samples (**Figure-7**). In this trial, a very significant amount of cleaved caspase-3 was observed for the Tm-PERK-KO and Tm-IRE1 $\alpha$ -KO cells, which backs up the data obtained in the previous three trials. In this case, the PERK-KO and IRE1 $\alpha$  -KO cell lines showed caspase-3 cleavage when treated with either toxin (Tg or Tm).

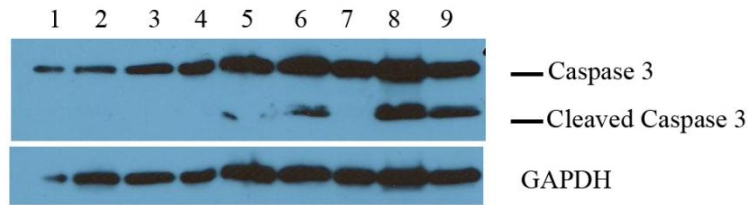


**Figure-7: Trial-4 Results for IRE1 $\alpha$ -KO and PERK-KO Samples.** Significant caspase-3 cleavage was observed in PERK-KO and IRE1 $\alpha$ -KO cells treated with Tm. (1) WT untreated, (2) IRE1 $\alpha$ -KO untreated, (3) PERK-KO untreated, (4) WT Tg treated, (5) IRE1 $\alpha$ -KO Tg treated, (6) PERK-KO Tg treated, (7) WT Tm treated, (8) IRE1 $\alpha$ -KO Tm treated, (9) PERK-KO Tm treated.

For all four trials, no cleavage of caspase-3 was observed for any of the ATF6 $\alpha$ -KO cells. This is a significant finding as it shows that the ATF6 $\alpha$  pathway is not as critical in murine fibroblast cells as the other pathways. In all cases, the ATF6 $\alpha$ -KO cells produced the same results as the wild type cells, showing that the ATF6 $\alpha$  pathway provides little help in relieving ER stress in the fibroblasts, so it is mostly the PERK and IRE1 $\alpha$  pathways. The PERK and IRE1 $\alpha$  pathways are concluded to be more important because when they are knocked out, cell death increases, so the cells were unable to relieve the stress in the absence of those two pathways. Although these two pathways appear to be important for the ER stress response in mouse embryonic fibroblasts, the results did not provide any conclusive evidence showing which of these two pathways are the more important of the two.

## DISCUSSION

The purpose of this project was to help identify which endoplasmic reticulum (ER) pathways are important in stress-related apoptosis. The hypothesis formed by the lab is that the ATF6 $\alpha$  pathway is not as important in embryonic mouse fibroblasts as it is in adult pancreatic  $\beta$ -cells. ER stress was induced in various KO embryonic fibroblast cell lines using toxins Tg and Tm, and the responses to the toxins were measured by immunoblots for caspase-2 (data not shown), caspase-3, and caspase-9 (data not shown), which are proteins related to apoptosis. The responses were measured in knockout and WT cell lines for PERK, IRE1 $\alpha$ , and ATF6 $\alpha$  transcription factor markers for key stress reduction pathways.

The main conclusion is that the ATF6 $\alpha$  pathway is not important for alleviating ER stress in mouse embryonic fibroblast cells, while IRE1 $\alpha$  and PERK pathways are. The results provide the first information on these pathways in embryonic fibroblasts. IRE1 $\alpha$  and PERK knockout cells showed cleaved Caspase-3, whereas the ATF6 $\alpha$  was no different than the Wild Type. **Figure-8** below summarizes the findings, showing which pathways are important in regulating ER stress in embryonic mouse fibroblasts (highlighted in green), and which pathway appears to not be involved (crossed out in red).

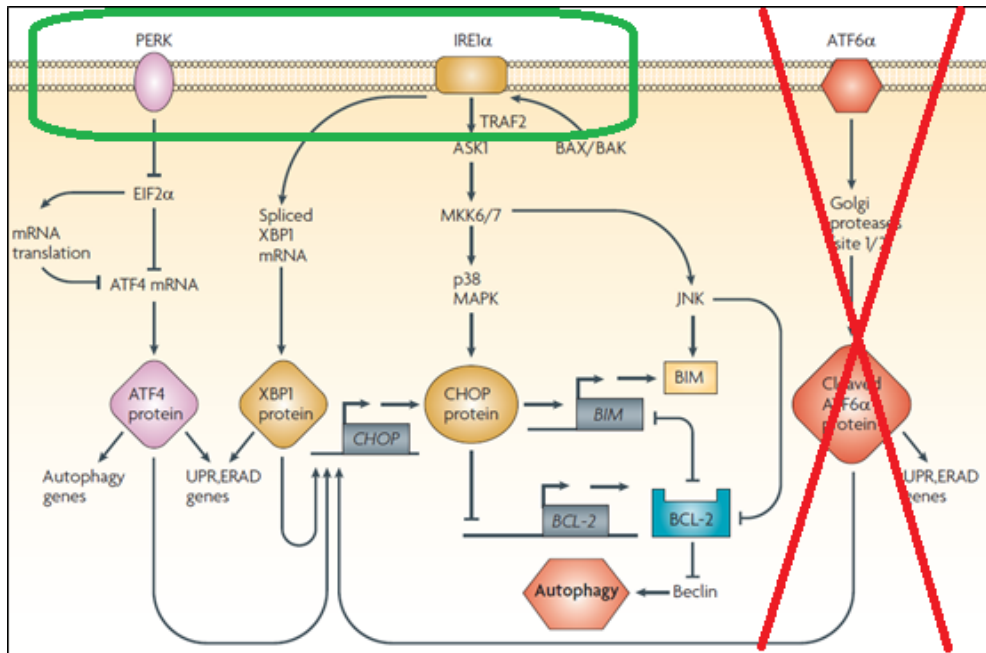


**Figure-8: Diagram of the Important UPR Pathways in Mouse Embryonic Fibroblast Cells.** This figure highlights the pathways that have been shown to be of more importance in regulating ER stress in embryonic mouse fibroblasts (highlighted in green) as well as indicating which pathway plays a lesser role in the regulation of ER stress (crossed off in red).

This data shows importantly that the ER stress reduction pathways change from early in life (embryonic fibroblasts) to later in life (adult pancreatic  $\beta$ -cells). The data also shows that embryonic mouse fibroblasts are more susceptible to stress caused by cell cycle arrest in the G1 phase, which is how the tunicamycin (Tg) induced stress in the cells.

Some of the problems that arose during the project were outdated protocols for pancreatic cells when embryonic cell protocols should have been used. Also, some of the Western blots did not show the proper bands or any bands at all, leading us to believe that there may have been something wrong with the specific antibodies used. Due to this we were unable to gather any conclusive data for the Caspase-2 and Caspase-9 antibodies.

There were several things that could have been done to increase the efficiency of the assays that we performed. The first was to decrease the dilutions for the antibodies being used, both primary and secondary. This would have allowed them to bind to the membrane better and would have fluoresced better once the membrane was visualized. We could also have tried loading more protein per lane for the gels. It is also possible that the antibodies that we used for Caspase-2, Caspase-9 or one of the secondary antibodies did not work as effectively as believed. Numerous Western Blots were performed, but the only data that was obtained for both Caspase-2 and Caspase-9 probes was inconclusive.

## **Perspectives**

This project extended the work of several of the papers cited in the Background section. Kim et al. (2008) provides a link between  $\beta$ -cell cell death and ER stress in the UPR, and specifically the function for each of the pathways that were also investigated in this project. Osowski and Urano (2010) provide the link between ER stress and the death of  $\beta$ -cells in relation to Wolfram patients. Rigoli et al. (2011) links the WFS1 mutations to effects on ATF6 $\alpha$  which plays a crucial role in the UPR for pancreatic  $\beta$ -cells. These three papers played a key role in setting the stage for this project.

## **Future Experiments**

Of the three pathways thought to be involved in the ER Unfolded Protein Response, ATF6 $\alpha$  has been shown to be the most important of the three pathways in pancreatic  $\beta$ -cells found later in life. However, our results have shown that the ATF6 $\alpha$  pathway is less important in embryonic mouse fibroblasts. This difference logically leads to the question of what is the timing

of this change in importance, as well as what causes this shift in significance. This alteration from fibroblasts to pancreatic  $\beta$ -cell might hold a clue that will aid in the resolution of the question of what is the mechanism of WFS1 when it is mutated and leads to ER stress, which in turn takes a part in Wolfram's syndrome.

An additional question to be resolved is if the pathways that regulate ER stress become defective, could they be stimulated so that they become effective again. Another possibility instead of stimulating the defective pathway could be to imitate the mechanism for the defective pathway, which would compensate for that pathway being defective. If the mechanisms for those pathways and their relationship to the mutation in WFS1 could be identified, it might be possible to provide a way to alleviate the ER stress caused by the disease and discover a way to help alleviate the symptoms of Wolfram's syndrome.

## BIBLIOGRAPHY

- Barrett T, and Bundley S. Wolfram (DIDMOAD) Syndrome. *J Med Genet*, 34 (1997): 838-841.
- Hamanaka R, Bennett B, Cullinan S, Diehl J. PERK and GCN2 Contribute to eIF2 Phosphorylation and Cell Cycle Arrest after Activation of the Unfolded Protein Response Pathway. *Molecular Biology of the Cell*, 16 (2005): 5493-5501.
- Inoue H, Tanizawa Y, Wasson J, Behn P, Kalidas K, Bernal-Mizrachi E, Mueckler M, Marshall H, Donis-Keller H, Crock P, et al. (1998) A gene encoding a transmembrane protein is mutated in patients with diabetes mellitus and optic atrophy (Wolfram syndrome). *Nature Genetics*, 20: 143–148.
- Kim I, Xu W, Reed J. Cell Death and Endoplasmic Reticulum Stress: Disease Relevance and Therapeutic Opportunities. *Drug Discovery*, 7 (2008): 1013-1030.
- Lee K, Dey M, et al. Structure of the Dual Enzyme Ire1 Reveals the Basis for Catalysis and Regulation in Nonconventional RNA Splicing. *Cell*, 132 (2008): 89-100.
- Minton J, Rainbow L, Ricketts C, Barrett T. Wolfram Syndrome. *Reviews in Endocrine & Metabolic Disorders*, 4 (2003): 53-59.
- Osowski CM, Urano F. The binary switch that controls the life and death decisions of ER stressed  $\beta$  cells. *Curr Opin Cell Biol*, doi:10.1016/j.ceb.2010.11.005.
- Rigoli L, Lombardo F, Di Bella C. Wolfram Syndrome and WFS1 Gene. *Clinical Genetics*, 79 (2011): 103–117.
- Schröder M. The Unfolded Protein Response. *Molecular Biotechnology*. 34 (2006): 279-290.
- Strom TM, Hortnagel K, Hofmann S, Gekeler F, Scharfe C, Rabl W, Gerbitz KD, and Meitinger T (1998) Diabetes insipidus, diabetes mellitus, optic atrophy and deafness (DIDMOAD) caused by mutations in a novel gene (wolframin) coding for a predicted transmembrane protein. *Human Molecular Genetics*, 7: 2021–2028.
- Takeda K, Inoue H, Tanizawa Y et al. Wfs1 (Wolfram syndrome1) Gene Product: Predominant Subcellular Localization to Endoplasmic Reticulum in Cultured Cells and Neuronal Expression in Rat Brain. *Human Molecular Genetics*, 10 (2001): 477–484.
- Thuerauf D, Morrison L, Glemotski C. Opposing Roles for ATF6 $\alpha$  and ATF6 $\beta$  in Endoplasmic Reticulum Stress Response Gene Induction. *The Journal of Biological Chemistry*, 279 (2004): 21078-21084.

Weitzman J. JNK. *Current Biology*, 10 (2000): R290.

Wolfram DJ and Wagener HP. Diabetes Mellitus and Simple Optic Atrophy Among Siblings: Report of Four Cases. *Mayo Clin. Proc.* 13 (1938): 715-718.